

# Centrifugal Compression of Crystal-like Structures of Deionized Colloidal Spheres

Tsuneo Okubo

Contribution from the Department of Polymer Chemistry, Kyoto University, Kyoto 606, Japan.  
Received May 22, 1989

**Abstract:** A new and convenient technique for the study of the elastic properties of the crystal-like structures of deionized colloidal spheres (85–173 nm in diameter) is developed by reflection spectrum measurements at centrifugal equilibrium. Beautiful iridescent color bands appear in the observation cell, and centrifugal compression occurs for the lattice spacings ( $D$ ) of the crystal-like structures a way from center. The  $D$  values are explained by the effective hard-sphere model; a colloidal sphere is coated with an electrical double layer. The elastic moduli ( $G$ ) for the ordered lattices are estimated to be between 50 and 800 Pa from the  $D$  values, as a function of the distance from the center of the cell.  $G$  increases as concentration increases and/or the size of the spheres decreases. The  $g$  factor, which is a parameter for the thermal fluctuation of a sphere in the colloidal crystals, is estimated to be between 0.01 and 0.1. The way  $D$  and  $G$  are influenced by sphere concentration shows that electrostatic intersphere repulsion and the elongated Debye screening length around the spheres are both essential to explain the appearance of the crystal-like structures.

Recently, keen attention has been paid to the extraordinary (gas-like, liquid-like, and crystal-like) suspension properties of "deionized" colloidal spheres. The two essentially important factors in the characteristic properties are an electrostatic interspherical repulsion and an elongated Debye screening length in the deionized state.<sup>1-17</sup> The ionic concentration of suspensions, which are deionized completely by mixed beds of cation- and anion-exchange resins, is very low, ca.  $2 \times 10^{-7}$  mol dm<sup>-3</sup> due to only H<sup>+</sup> and OH<sup>-</sup> from water dissociation. The Debye length for the completely deionized suspensions is significantly long, to the order of micrometers. Sheaths of double layers, the widths of which are approximately equal to the Debye length, are very soft and can be compressed easily or distorted by an external force.

According to the effective hard-sphere model, "crystallike" ordering is formed when the effective diameter ( $D_{\text{eff}}$ ) of the spheres, which includes the Debye screening length ( $D_1$ ), is close to or longer than the mean intersphere distance ( $D_0$ ), i.e.,  $D_{\text{eff}} [=2D_1 + \text{diameter} (d_0)] \geq D_0$ . In crystal-like structures, the spheres fluctuate around their equilibrium points. When  $D_{\text{eff}}$  is comparable to or a bit shorter than the  $D_0$  value, the distribution of the spheres is usually "liquid-like" and they move without keeping their positions, though the effective concentration is much higher than the stoichiometric concentration due to the effect of the elongated Debye length. When  $D_{\text{eff}}$  is much shorter than  $D_0$ ,

Table I. Properties of Spheres Used

sphere	diam, nm	charge density, $\mu\text{C}/\text{cm}^2$	
		strongly acidic	weakly acidic
D1C25	85 $\pm$ 6	1.5	1.0
D1C27	91 $\pm$ 6	2.0	1.4
D1B76	109 $\pm$ 3	2.1	0.71
D1K88	137 $\pm$ 16	0.58	0.60
D1B72	173 $\pm$ 7	1.0	

a "gas-like" distribution is observed. Thus, the Debye screening length is essentially the important factor for explaining the characteristic properties, and the difference between  $D_{\text{eff}}$  and  $D_0$  gives a very useful criterion with which to distinguish the three structures of deionized spheres from each other.

The elastic moduli of crystal-like structures of deionized colloidal suspensions have been determined by Crandall and Williams,<sup>6</sup> Mitaku et al.,<sup>8,18,19</sup> Lindsay and Chaikin,<sup>11</sup> and this author.<sup>16</sup> The elastic modulus of a colloidal crystal is proportional to the number density of the spheres and the intersphere electrostatic repulsive energy. Therefore, there is no essential difference between colloidal systems and metals, plastic crystals, viruses, etc. in view of the magnitudes of their moduli.<sup>18,19</sup>

In order to study the main reasons for the occurrence of the crystal-like structures, the following sections discuss in detail the elastic modulus of crystal-like colloids, which is determined by using a unique and convenient technique, the reflection spectrum method at the centrifugal equilibrium. By rotating a quartz glass disk containing colloidal suspension, beautiful iridescent color bands due to Bragg diffraction from the asymmetric and compressed crystals are seen.

The reflection spectrum method provides information on the distance between two-dimensional parallel layers in ordered lattices and is especially effective for detecting small changes in lattice structures.<sup>1,4,20-22</sup> The lattice spacings ( $D$ , intersphere distance) were determined from the wavelength at the sharp reflection peaks.<sup>23</sup> Face-centered cubic (fcc) and body-centered cubic (bcc) lattices were imputed to coexist in the deionized suspensions. The fcc distribution was more stable at higher concentrations than the

- (1) Luck, W.; Klier, M.; Wesslau, H. *Ber. Bunsenges. Phys. Chem.* **1963**, *67*, 75, 84.
- (2) Stone-Masui, J.; Watillon, A. *J. Colloid Interface Sci.* **1968**, *28*, 187.
- (3) Vanderhoff, J. W.; van de Hul, H. J.; Tausk, R. J. M.; Overbeek, J. Th. G. *Clean Surfaces: Their Preparation and Characterization for Interfacial Studies*; Goldfinger, G., Ed.; Dekker: New York, 1970.
- (4) Hiltner, P. A.; Papir, Y. S.; Krieger, I. M. *J. Phys. Chem.* **1971**, *75*, 1881.
- (5) Kose, A.; Ozaki, M.; Takano, K.; Kobayashi, Y.; Hachisu, S. *J. Colloid Interface Sci.* **1973**, *44*, 330.
- (6) Crandall, R. S.; Williams, R. *Science* **1977**, *198*, 293.
- (7) Schaefer, D. W. *J. Chem. Phys.* **1977**, *66*, 3980.
- (8) Mitaku, S.; Otsuki, T.; Okano, K. *Jpn. J. Appl. Phys.* **1978**, *17*, 305, 627.
- (9) Clark, N. A.; Hurd, A. J.; Ackerson, B. J. *Nature (London)* **1979**, *281*, 57.
- (10) Goodwin, J. W.; Ottewill, R. H.; Parentich, A. *J. Phys. Chem.* **1980**, *84*, 1580.
- (11) Lindsay, H. M.; Chaikin, P. M. *J. Chem. Phys.* **1982**, *76*, 3774.
- (12) Hansen, J. P.; Haytor, J. B. *Mol. Phys.* **1982**, *46*, 651.
- (13) Tomita, M.; Takano, K.; van de Ven, T. G. M. *J. Colloid Interface Sci.* **1983**, *92*, 367.
- (14) Pieranski, P. *Contemp. Phys.* **1983**, *24*, 25.
- (15) Hartl, W.; Versmold, H. *J. Chem. Phys.* **1984**, *81*, 2507.
- (16) Okubo, T. *Acc. Chem. Res.* **1988**, *21*, 281.
- (17) Ottewill, R. H. *Langmuir* **1989**, *5*, 4.

- (18) Mitaku, S.; Otsuki, T.; Okano, K. *Jpn. J. Appl. Phys.* **1980**, *19*, 439.
- (19) Mitaku, S.; Otsuki, T.; Kishimoto, A.; Okano, K. *Biophys. Chem.* **1980**, *71*, 411.
- (20) Fujita, H.; Ametani, K. *Jpn. J. Appl. Phys.* **1979**, *18*, 753.
- (21) Tomita, M.; van de Ven, T. G. M. *J. Colloid Interface Sci.* **1984**, *99*, 374.
- (22) Tomita, M.; van de Ven, T. G. M. *J. Phys. Chem.* **1985**, *89*, 1291.
- (23) Okubo, T. *J. Chem. Soc., Faraday Trans. 1* **1986**, *82*, 3163.

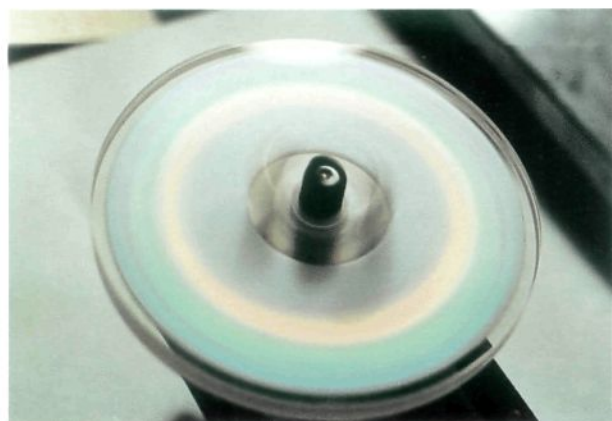


**Figure 1.** Photographs showing the rotating observation cell. D1K88 suspension 5 days after the sample was set.  $[D1K88]_0 = 0.0617$  in volume fraction. (a, top) Close-up picture was taken with an obtuse angle illumination, (b, bottom) Close-up picture was taken with an acute angle illumination.

bcc, and the latter often appeared at a high suspension temperature and in the presence of small amounts of a foreign salt. Electrically induced changes in the lattice structure have been studied by time-resolved reflection spectrum measurements.<sup>24</sup> The elastic moduli of the crystals were evaluated from the magnitude of the reflection peak shift as a function of electric field strength. The crystal-like structures were analyzed by the reflection spectrum method in the presence of neutral water-soluble polymers.<sup>25</sup> Recently, the time-resolved transmitted light and reflection spectra were obtained during the reappearance of the crystal-like structure after rapid flow through a thin optical flow cell.<sup>26</sup> Deformation of the crystal-like structure has also been studied under shear using a flow cell.<sup>27</sup> Furthermore, the effect of pressure,<sup>28</sup> an alternating field,<sup>29</sup> and the gravitational field<sup>30</sup> on the crystal-like ordering have been studied by the reflection spectrum method.

### Experimental Section

**Materials.** D1C25, D1C27, D1B76, D1K88, and D1B72 were monodisperse polystyrene spheres purchased from Dow Chemical Co. The diameters and monodispersities, which were determined by the manufacturer by electron microscopy, are listed in Table I. The charge densities of strongly acidic (sulfate ions) and weakly acidic (carboxylic acid) ionic groups were determined by conductometric titration with an autobalance precision bridge, Model B331 Mark II (Wayne Kerr Lab., Bognor Regis, Sussex, U.K.). The spheres were carefully purified several

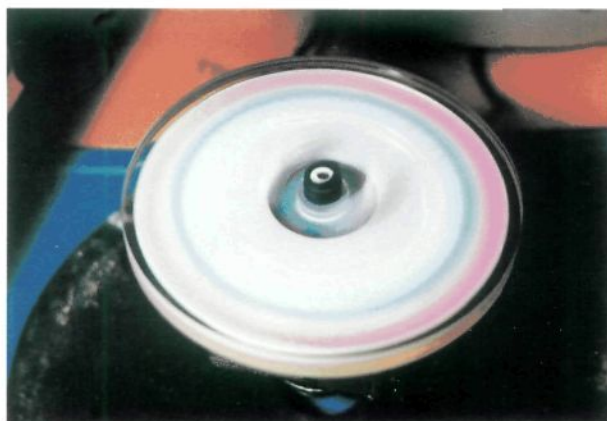


**Figure 2.** (a, top) Photograph showing a rotating observation cell. D1B72 suspension 5 days after the sample was set.  $[D1B72]_0 = 0.0820$ ; Close-up picture was taken with an acute angle illumination. (b, bottom) Photograph showing the observation cell on black and white color papers. After the reflection spectra were taken at the centrifugal equilibrium, the cell was detached from the driving motor and the close-up picture was taken with zero angle illumination.

times by an ultrafiltration cell (Model 202; membrane, Diaflo XM300; Amicon Co., Lexington, MA), and the samples were then treated with a mixed bed of cation- and anion-exchange resins (Bio-Rad, AG501-X8(D), 20–50 mesh) for more than 10 days. The resulting suspension was believed to contain only the macroions (spheres) and their counterions ( $H^+$ ), and  $H^+$  and  $OH^-$  from water dissociation. Water used for the purification and for suspension preparations was deionized by using cation- and anion-exchange resins (Puric-R, type G10, Organo Co., Tokyo) and purified further by a Milli-Q reagent-grade water system (Millipore Co., Bedford, MA).

**Reflection Spectrum Measurements at the Centrifugal Equilibrium.** The observation cell was made from a quartz glass disk (80 mm in diameter and 1 mm in width) with two stoppers. A purified suspension of  $5\text{ cm}^3$  volume was introduced into the cell. The cell was rotated horizontally at 3430 rpm for 5–7 days until the centrifugal equilibrium was attained. The reflection spectra at various distances from the center, at an incident angle of  $90^\circ$ , were recorded on a multichannel photodetector (MCPD-110B, Otsuka Electronics, Hirakata, Osaka) connected to a Y-type optical-fiber cable. The instrument was operated by a microcomputer (MC800, Otsuka Electronics). The camera used to take close-up pictures was a Nikon FE2 with a zoom close-up lens (Kenko Co., Tokyo).

### Results

**Crystal-like Colloids at the Centrifugal Equilibrium.** When the samples were set in the cell, we often observed brilliant and sparkling patches. These patches are called "crystallites" or "islands". Vanderhoff et al.<sup>3</sup> first reported the existence of the ordered region of liquid crystals or crystallites for monodisperse polystyrene spheres in deionized suspension. These crystallites seemed to flicker but disappeared immediately when the suspension was shaken. However, they reappeared within several seconds

(24) Okubo, T. *J. Chem. Soc., Faraday Trans. 1* **1987**, *83*, 2487.  
 (25) Okubo, T. *J. Chem. Soc., Faraday Trans. 1* **1987**, *83*, 2497.  
 (26) Okubo, T. *J. Chem. Soc., Faraday Trans. 1* **1988**, *84*, 1163.  
 (27) Okubo, T. *J. Chem. Soc., Faraday Trans. 1* **1988**, *84*, 1171.  
 (28) Okubo, T. *J. Chem. Soc., Faraday Trans. 1* **1988**, *84*, 1949.  
 (29) Okubo, T. *J. Chem. Soc., Faraday Trans. 1* **1988**, *84*, 3377.  
 (30) Okubo, T. *J. Chem. Soc., Faraday Trans. 1* **1989**, *85*, 455.

when the suspension was left to stand. The size of the crystallites was 0.1–0.5 mm in many cases and increased as the concentration of the spheres decreased.<sup>23,31</sup> Note that crystallites for the suspensions of high concentrations were often too small to be recognized with the naked eye, and the suspensions were transparent and iridescent. Sharp transitions from the crystal-like to liquid-like structures were observed in the transmitted light and reflection spectra when the deionized colloidal suspensions were diluted or foreign salt was added. The concentration for the transition of D1C25 spheres was 0.0054 in volume fraction, for example.<sup>32</sup> Iridescent color was clearly observed for the suspensions showing liquid-like structures. Iridescent color is, therefore, not convenient to distinguish liquid-like and crystal-like structures.

In the first 1 or 2 days of the observation cell rotation, the iridescent color bands appeared. Typical examples are shown in Figure 1. The color bands shown in Figure 1a indicate that the crystal-like structures for the outer part of the cell are compressed very strongly by the centrifugal field. Interestingly, complimentary colors appeared when angles between illumination and observation light were changed from obtuse to acute, as is clearly shown in Figure 1a and b. The centrifugal equilibrium was ascertained from the reflection spectrum measurements and was attained after 5–7 days of cell rotation.

Figure 2a shows the iridescent colors (with an obtuse angle) of the cell 5 days after the cell was set on the driving motor and rotated. Beautiful color bands appeared usually after 1 day. The suspension looked opaque, since the spheres were largest among the samples examined. For D1C25, D1C27, and D1B76 spheres, however, the suspensions were much more transparent. Figure 2b shows the cell that was taken off the motor after the centrifugal equilibrium state was attained. A significant color difference due to the reflection and transmitted lights was observed by placing the cell on a black and white background; see Figure 2b.

**Reflection Spectra and Lattice Spacings of Crystal-like Colloids at the Centrifugal Equilibrium.** In the reflection spectrum measurements the incident light hits the surface of the sample cell at right angles. When the cell contains an "ordered" colloidal suspension the light is turned back by Bragg diffraction. This corresponds to the reflection spectrum. Generally speaking, the shape of a reflection spectrum pattern is a single peak, a double peak, or a single peak with a shoulder. The two-wavelength peaks were always close together, with a difference of only 1.03 in the ratios of their wavelengths. This difference supports the idea that the peak appearing at the longer wavelength may be ascribed to the fcc lattice, while the shorter wavelength peak corresponds to the bcc lattices in the crystal-like structures. By use of a simple theoretical calculation, the ratio of the nearest-neighbor Bragg distance for fcc lattices to that for bcc lattices was found to be 1.0284 at the same sphere concentration. The intersphere spacing ( $D$ ) was determined from the peak wavelength.<sup>21</sup> For both fcc and bcc lattices, the distance  $D$  at a scattering angle of  $90^\circ$  is given by

$$D = 0.6124(\lambda_m/n_s) \quad (1)$$

where  $n_s$  is the refractive index of the sphere suspension (taken as that of water in this work) and  $\lambda_m$  is the peak wavelength.

Figure 3 shows the reflection spectra of D1B76 spheres at a distance from the disk center ( $R$ ) of 3.38 cm at various times during cell rotation. These reflection peaks are assigned to the fcc structures, and the wavelengths of the peaks are 637, 635, 618, 588.5, 575, and 565.5 nm, after 5 min, 2 h, 7 h, 1 day, 2 days, and 4 days, respectively.  $D$  values are, therefore, estimated from eq 1 to be 293, 292, 284, 270.5, 264, and 260 nm, respectively. Clearly, the lattice spacing at  $R = 3.38$  cm decreased with time. The compression of the lattice structures by the centrifugal field is obvious. Generally speaking, the crystal-like structure were kept throughout the suspension in the observation cell, though the lattice spacing increased as  $R$  decreased. However, the inner part of the suspension in the cell became liquid-like when the initial

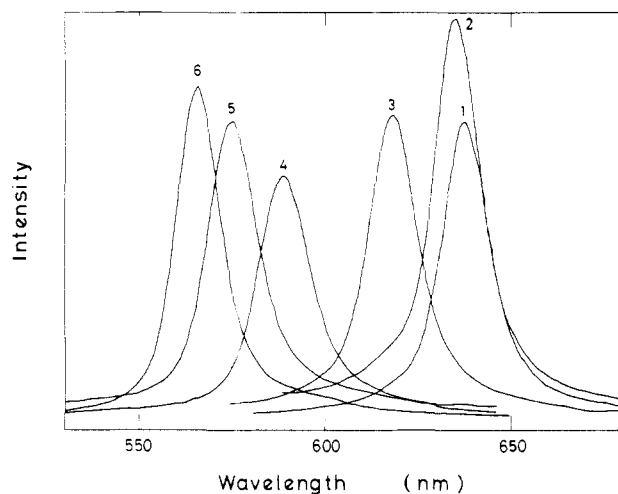


Figure 3. Changes in the reflection spectra for D1B76 suspensions after rotation of the cell starts.  $[D1B76]_0 = 0.0319$ ,  $R = 3.38$  cm. Curve 1, after 5 min; 2, 2 h; 3, 7 h; 4, 1 day; 5, 2 days; 6, 4 days.

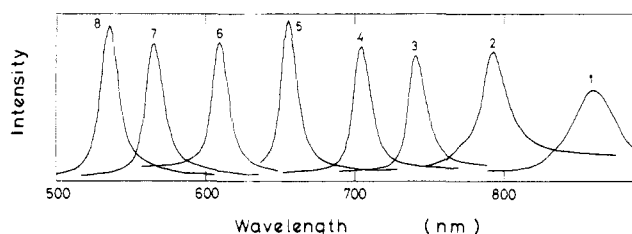


Figure 4. Reflection spectra of D1B76 suspension at various  $R$  values at the centrifugal equilibrium.  $[D1B76]_0 = 0.0319$ , 4 days after the cell was set. Curve 1,  $R = 0.88$  cm; 2, 1.48 cm; 3, 1.88 cm; 4, 2.18 cm; 5, 2.58 cm; 6, 2.98 cm; 7, 3.38 cm; 8, 3.68 cm.

sphere concentrations were low and/or the size of spheres is large. This is because the intersphere distances in the inner part often become larger than the critical distance,  $D_{\text{eff}} (= d_0 + 2D_1)$ . It is surprising to observe that the lattice spacing decreases sharply as  $R$  increases even for very small colloidal spheres, where the thermal motion of the spheres is so vigorous as to prevent an anisotropic distribution forming. The main reason for the changes in  $D$  are ascribed to the fact that free movement of the spheres in a crystallite is restricted strongly, so that the crystallite behaves as a unit of thermal movement.

Figure 4 shows the reflection spectra of D1B76 spheres at various  $R$ 's at the centrifugal equilibrium, which was attained after 4 days of cell rotation. These reflection peaks are assigned to fcc structures. The single peak was obtained in the reflection spectra and the peak wavelength decreased significantly as  $R$  increased. However, the reflection peaks for the inner suspensions were rather broad. This will be partly due to the fact that the intersphere distances for the suspensions are close to the critical distance,  $D_{\text{eff}}$ , and due to the fact that the crystal-like structures transform from fcc to bcc lattices with the dilution of the suspension.

Figure 5 shows the changes of  $\lambda_m$  and  $D$  with time for D1B76 spheres at various  $R$  values. The open circles indicate the data 5 min after the rotation started, and the lattice spacing remained constant irrespective of the  $R$  values. The state of centrifugal equilibrium was attained after 5 days, as is seen in this figure, and both  $\lambda_m$  and  $D$  decreased sharply as  $R$  increased. Figures 6 and 7 shows the  $\lambda_m$  and  $D$  values at the centrifugal equilibrium for other systems. The decreasing tendency of  $\lambda_m$  or  $D$  with  $R$  was more substantial for the suspensions of lower elastic moduli. The discontinuity in the curves of  $\lambda_m$  (or  $D$ ) vs  $R$  plots, which was observed for D1K88 spheres (see Figure 7), is due to the transformation of the crystal-like structures from fcc to bcc lattices with decreasing  $R$ .

Time-resolved reflection spectra for D1C25 spheres were obtained (Figure 8) after the rotation of the observation cell was stopped. Clearly, the reflection peaks became sharper with time

(31) Okubo, T. *Ber. Bunsenges. Phys. Chem.* **1987**, *91*, 516.

(32) Okubo, T. *J. Chem. Soc., Faraday Trans.*, in press.

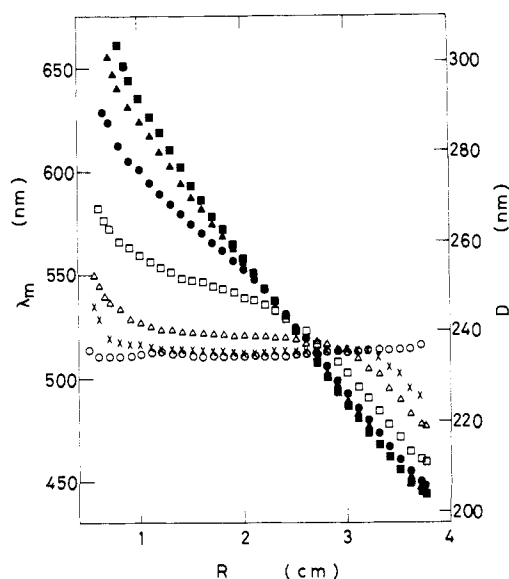


Figure 5. Changes in  $\lambda_m$  and  $D$  for D1B76 suspension at various  $R$  values after the cell was set.  $[D1B76]_0 = 0.0637$ ; O, after 5 min; X, 3 h;  $\Delta$ , 8 h;  $\square$ , 1 day;  $\bullet$ , 2 days;  $\blacktriangle$ , 3 days;  $\blacksquare$ , 5 days.

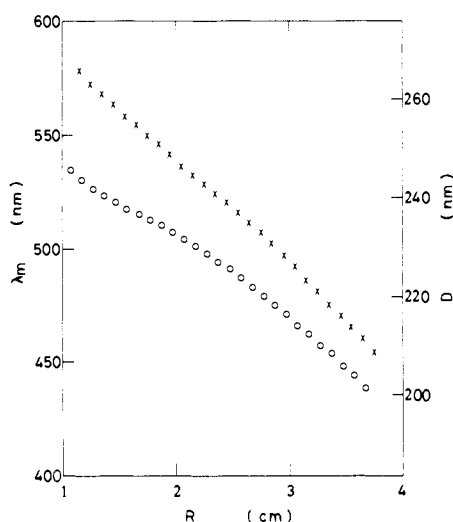


Figure 6. Changes in  $\lambda_m$  and  $D$  for D1C25 (O) and D1C27 (X) suspensions at various  $R$  values at the centrifugal equilibrium.  $[D1C25]_0 = 0.0179$ ,  $[D1C27]_0 = 0.0296$ .

and the intensity became strong. In this experiment, the spectra were not taken until 5 days after the cell was detached from the motor. It took a longer time to attain the equilibrium state. During rotation of the cell, the suspension must be perturbed, though slightly, by the mechanical vibration caused by the electric motor. Then, the crystal-like structures will be in a metastable state. When the rotation is stopped, formation of the very stable crystal-like structures proceeds. In our previous papers,<sup>26,33,34</sup> the local rearrangement times (or structural relaxation times) for strongly interacting (repulsive) spheres were of two kinds: fast (5–50 ms) and slow (1 s or longer). The fast-decaying mode is related to the translational diffusion process of the spheres, and the slow mode is designated as the fluctuation of crystallites and/or their grain boundaries in the state of strong interaction between spheres and the glass plane of the cell. It is highly plausible that it takes a very long time, on the order of days, for the formation of the very stable crystals.

#### Discussion

As was described in the introduction, the effective hard-sphere model tells us that crystal-like ordering is formed within a very

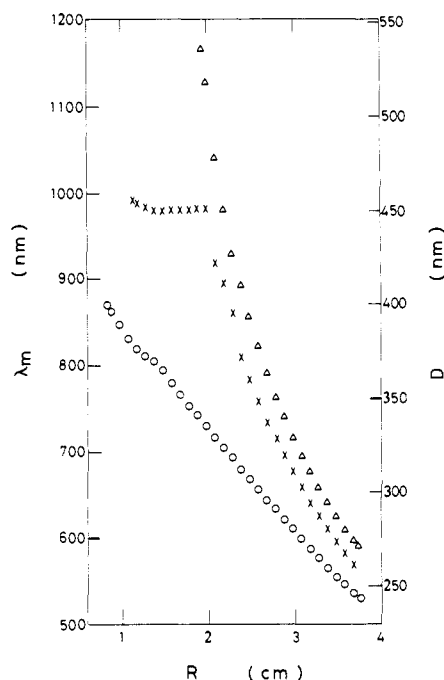


Figure 7. Changes in  $\lambda_m$  and  $D$  for D1B76 (O), D1K88 (X), and D1B72 ( $\Delta$ ) suspensions at various  $R$  values at the centrifugal equilibrium.  $[D1B76]_0 = 0.0319$ ,  $[D1K88]_0 = 0.0617$ ,  $[D1B72]_0 = 0.0820$ .

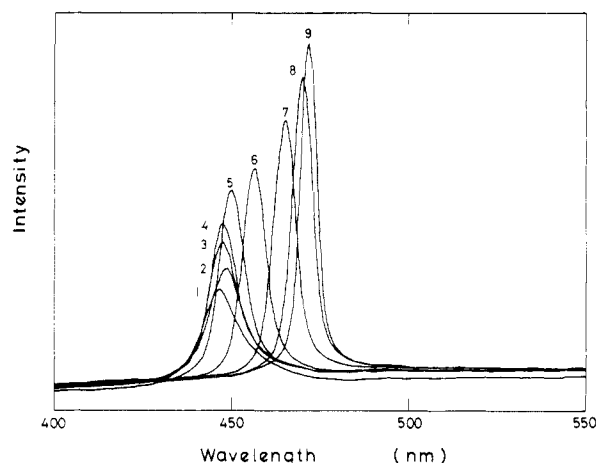


Figure 8. Changes in the reflection spectra for D1C25 suspensions after the cell was set.  $[D1C25]_0 = 0.0179$ ,  $R = 3.48$  cm; curve 1, after 5 min; 2, 10 min; 3, 30 min; 4, 1 h; 5, 3 h; 6, 9 h; 7, 1 day; 8, 2 days; 9, 5 days.

short time, corresponding to the structural relaxation time when the effective diameter of a sphere, including Debye screening length, is long as compared with the mean intersphere distance. In order to account for the observed  $D$  values by this model, the Debye length was estimated in the absence of foreign salt.  $D_1$  is given by

$$D_1 = (4\pi e^2 n / \epsilon k_B T)^{-1/2} \quad (2)$$

where  $e$  is the electronic charge,  $\epsilon$  is the dielectric constant of the solvent,  $k_B$  is the Boltzmann constant, and  $n$  is the concentration of free cations ( $H^+$ ) and anions ( $OH^-$ ) in deionized suspension, given by  $n = n_c + n_0$ , where  $n_c$  is the concentration (number of ions per  $cm^3$ ) of diffusible counterions and  $n_0$  is the concentration of both  $H^+$  and  $OH^-$  from the dissociations of water. In this work  $n_0$  was taken to be  $2 \times 10^7 \text{ mol dm}^{-3} \times N_A \times 10^{-3} \text{ cm}^{-3}$ , where  $N_A$  is Avogadro's number. In order to estimate  $n_c$ , the fraction of free counterions ( $\beta$ ) must be known. Values of  $\beta$  have been determined for colloidal spheres of various sizes and charge densities.<sup>3,35–37</sup>  $\beta$  for D1B76 spheres, for example, was estimated

(33) Okubo, T. *J. Chem. Phys.* **1987**, *87*, 3022.

(34) Okubo, T. *J. Colloid Interface Sci.* **1987**, *117*, 165.

(35) Alexander, S.; Chaikin, P. M.; Grant, P.; Morales, G. J.; Pincus, P.; Hone, D. *J. Chem. Phys.* **1984**, *80*, 5776.

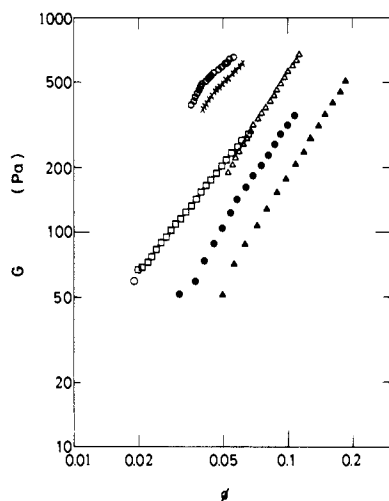


**Figure 9.** Plots of  $\log G$  against  $\log \phi$  for D1C25 (O), D1C27 (X), D1B76 ( $\Delta$ ,  $\square$ ), D1K88 ( $\bullet$ ), and D1B72 ( $\blacktriangle$ ) suspensions.  $[D1C25]_0 = 0.0179$ ,  $[D1C27]_0 = 0.0296$ ,  $[D1B76]_0 = 0.0637$  ( $\Delta$ ),  $[D1B76]_0 = 0.0319$  ( $\square$ ),  $[D1K88]_0 = 0.0617$ ,  $[D1B72]_0 = 0.0820$ .

to be 0.05. The concentrations of spheres at the peaks 1–6 in Figure 4 are estimated by using eq 3 to be 0.0382, 0.0386, 0.0418, 0.0485, 0.0519, and 0.0546 in volume fraction ( $\phi$ ), respectively.

$$\phi = (9.136d_0/\lambda_m)^3 \quad (3)$$

$D_1$  values were calculated as 89.5, 89.1, 85.6, 79.5, 76.8 and 74.9 nm, respectively. Thus, the effective diameters,  $D_{\text{eff}}$ , are 288, 287, 280, 268, 263, and 259 nm, respectively. The values of  $D_{\text{eff}}$  agree well with the corresponding  $D$  values (293, 292, 284, 270.5, 264, and 260 nm, respectively) within the experimental and theoretical uncertainties. A more systematic comparison of  $D$  and  $D_{\text{eff}}$  has been made for various spheres and concentrations,<sup>38–41</sup> and the agreement was satisfactory. This equality supports the validity of the effective hard-sphere model and indicates that the electrostatic intersphere repulsion is essential for ordering.

The decrease in lattice spacing with  $R$  demonstrates that the centrifugal field produces an elastic deformation. Because of the asymmetric distribution of spheres, the summation of forces between a reference sphere and all the neighboring spheres yields a repulsive force, which is counterbalanced by the centrifugal force under thermal diffusion. The repulsive force,  $F_1$ , due to the deformation of the elastic crystals at the distance from the center of the cell,  $R(I)$ , is given by eq 4, where  $G$  is the elastic modulus

$$F_1 = -G[(D(N) - D(1))/D(1)]R(N)\theta l \quad (4)$$

(rigidity), and  $D(I)$  is the lattice spacing at  $R(I)$ .  $I = 1$  and  $N$  denote the innermost point and an arbitrary point of the suspension in the cell.  $\theta$  is an arbitrary small central angle;  $l$  is the width of the observation cell. On the other hand, the centrifugal force applied on the suspension ( $F_2$ ) is given by eq 5, where  $\omega$  is the

$$F_2 = \omega^2(\rho - \rho_0)\theta \sum_{I=2}^{N-1} \{\phi(I)R(I)^2[R(I) - R(I-1)]\} \quad (5)$$

angular velocity,  $\rho$  and  $\rho_0$  are the specific gravities of the spheres and that of the solvent.  $\phi(I)$  is the concentration of the spheres in volume fraction at point  $R(I)$  and given by eq 3. From the equality,  $F_1 = F_2$  at the centrifugal equilibrium,  $G(N)$  is given as

$$G(N) = \{[\omega^2(\rho - \rho_0)D(1)]/[R(N) \times [D(N) - D(1)]]\} \sum_{I=2}^{N-1} \{\phi(I)R(I)^2[R(I) - R(I-1)]\} \quad (6)$$

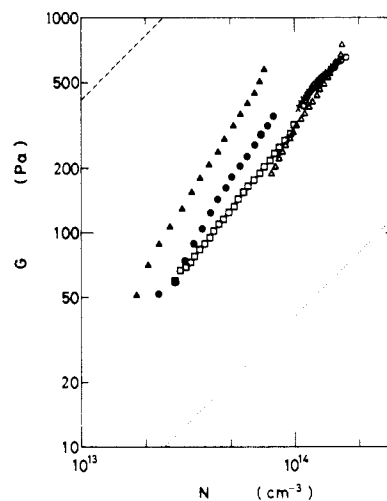


**Figure 10.** Plots of  $\log G$  against  $\log N$  for D1C25 (O), D1C27 (X), D1B76 ( $\Delta$ ,  $\square$ ), D1K88 ( $\bullet$ ), and D1B72 ( $\blacktriangle$ ) suspensions. Concentrations of the spheres are the same as Figure 9.  $\cdots$ ,  $g = 0.1$ ;  $---$ ,  $g = 0.01$ .

Figure 9 shows the  $G$  values thus estimated from the experimental data of  $D$  shown in Figures 5–7. Clearly, (1)  $G$  values were between 50 and 800 Pa, (2)  $\log G$  increased with the slope of unity as  $\log \phi$  increased, and (3)  $G$  increased as the sphere's size decreased at the same  $\phi$ .

The order of magnitude of  $G$  may be written in terms of the magnitude of the thermal fluctuation  $\delta$  of a sphere as<sup>6,18,19</sup>

$$G \approx f/D \approx (k_B T / \langle \delta^2 \rangle) / D \quad (7)$$

where  $f$  is the force constant. Introducing a nondimensional parameter  $g$  for  $\langle \delta^2 \rangle^{1/2} / D$ , the modulus is obtained as a linear function of number density of spheres,  $N$ :

$$G \approx Nk_B T / g^2 \quad (8)$$

When  $g = 1$ , eq 8 gives the elastic modulus of an ideal gas having the same sphere concentration. Lindemann's law of crystal melting tells us that  $g < 0.1$  holds for a stable crystal.

Figure 10 shows the plots of  $\log G$  against  $\log N$ . The dotted and dashed lines in the figure represent the values of  $G$  when  $g = 0.1$  and 0.01, respectively. Clearly,  $G$  values are located between the dotted and dashed lines. In these plots,  $G$  values seem to be located at the same place irrespective of the sphere's size. It should be noted here that most  $G$  values obtained so far for the deionized colloidal suspensions are also located between the dotted and dashed lines.<sup>3,11,18,19,24,30,39,42–45</sup> Note that eq 8 means that the elastic moduli of the colloidal crystals are proportional to the number density of the spheres to a first approximation, and there is no essential difference between colloidal systems, metals, plastic crystals, etc. in terms of the magnitudes of their moduli.<sup>18,19</sup> The absolute values of the elastic moduli differ from each other depending on the Coulombic repulsion between the spheres as is given by eq 9,<sup>6,11,46</sup> where  $U$  is the electrostatic repulsion energy between

$$G \approx NU \quad (9)$$

two spheres. Note further that the magnitude of  $G$  is highly sensitive to the charge density and monodispersity in the sizes of the colloidal spheres.

**Acknowledgment.** The author thanks Dr. J. Yamanaka for his useful suggestions. This work was supported by grants-in-aid from the Japanese Ministry of Education, Science and Culture, the Kurata Foundation, and the Nippon Sheet Glass Co.

Registry No. Polystyrene, 9003-53-6.

(36) Okubo, T. *Ber. Bunsenges. Phys. Chem.* **1987**, *91*, 1064.

(37) Okubo, T. *J. Colloid Interface Sci.* **1988**, *125*, 380.

(38) Okubo, T. *J. Chem. Soc., Faraday Trans. 1* **1986**, *82*, 3185.

(39) Okubo, T. *J. Chem. Phys.* **1987**, *86*, 2394.

(40) Okubo, T. *J. Chem. Phys.* **1987**, *86*, 5182.

(41) Okubo, T. *J. Chem. Phys.* **1989**, *90*, 2408.

(42) Okubo, T. *Colloid Polym. Sci.* **1987**, *265*, 522.

(43) Okubo, T. *J. Chem. Phys.* **1988**, *88*, 658.

(44) Okubo, T. *J. Chem. Phys.* **1988**, *88*, 2083.

(45) Okubo, T. *Ber. Bunsenges. Phys. Chem.* **1988**, *92*, 504.

(46) Morad, M.; Koch, A. J.; Rothen, F. *J. Phys.* **1986**, *47*, 217.